Engineering the magnetocaloric properties of PrVO 3 epitaxial oxide thin films by strain effects

Hamza Bouhani, Asmaa Endichi, Deepac Kumar, O. Copie, Halima Zaari, Adrian David, Arnaud Fouchet, Wilfrid Prellier, Omar Mounkachi, Mohamed Balli, et al.

Engineering the magnetocaloric properties of epitaxial oxide thin films by strain effects

Hamza Bouhani, Asmaa Endichi, Deepac Kumar, Olivier Copie, Halima Zaari, Wilfrid Prellier, Adrian David, Arnaud Fouchet, Omar Mounkachi, Mohamed Balli, Abdelilah Benyoussef, Abdallah El Kenz and Stéphane Mangin*

Dr. H. Bouhani, Dr. A. Endichi Dr. O. Copie, Prof. S. Mangin
Institut Jean Lamour
UMR 7198 CNRS-Université de Lorraine F-54000, France

Dr. H. Bouhani, Dr. A. Endichi, Dr. H. Zaari, Pr. O. Mounkachi, Prof. A. Benyoussef, Prof A. El. Kenz.
Laboratory of Condensed Matter and Interdisciplinary Sciences (LaMCScI)
Faculty of Science, Mohammed V University, 1014 Rabat, Morocco

Dr. D. Kumar Dr. A. David, Dr A. Fouchet, Dr. W. Prellier
Normandie Univ.
ENSICAEN UNICAEN
CNRS, CRISMAT
6 Boulevard Maréchal Juin, F-14050 Caen, Cedex 4, France

Pr. Dr. M. Balli*
LERMA, ESIE
International University of Rabat
Parc Technopolis, Rocade de Rabat-Salé, 11100, Morocco

*mohamed.balli@uir.ac.ma

Keywords: strain engineering, magnetic refrigeration, perovskites, strongly correlated oxides, thin films

In this paper, we demonstrate how strain effects can be used to markedly tailor the magnetic and magnetocaloric properties of $PrVO_3$ thin films. The selection of appropriate thickness and substrate enables us to dramatically decrease the coercive magnetic field from 2.4 T previously observed in sintered PVO_3 bulk to 0.05 T for compressive thin films making from the $PrVO_3$ compound a nearly soft magnet. This is associated with a marked enhancement of the magnetic moment and the magnetocaloric effect that reach unusual maximum values of roughly 4.86 μ_B and 56.8 J/kg K in the magnetic field change of 6 T applied in the sample plane at the cryogenic temperature range (3 K), respectively. Our

calculations based on the Density Functional Theory (DFT) confirm the ground state and the enhancement of magnetic interactions via compressive strains in $PrVO_3$ thin films.

The interplay between several degrees of freedom in complex functional materials gained a lot of interest due to its potential to enhance the caloric effects in new alternative cooling technologies such as magnetic cooling [1-6]. The latter which is based on the magnetocaloric effect (MCE) is an emergent, innovating and potentially low carbon technology [7-8]. The MCE which is an intrinsic property of certain magnetic materials results in a change of their thermal state when subjected to an external magnetic field. Currently, Gadolinium Gd is the magnetic material used in the vast majority of magnetic cooling prototypes, mainly due to its magnetic phase transition taking place at 294 K leading to excellent magnetocaloric properties close to room temperature [9]. However, this metal presents multiple disadvantages such as its easy oxidation as well as the limitation of its working temperature range close to the room temperature. In addition, gadolinium cannot be used in large scale applications because of its high cost. These issues have motivated the scientists to search for cheaper, safe and performant magnetocaloric materials under moderate magnetic fields including intermetallic and oxides [8-9]. The magnetocaloric effect in manganite-based perovskites exhibiting multiferroic behaviors have become an interesting topic because of the potential application of these oxides in some specific applications such as the liquefaction of hydrogen and space industry. This sort of compounds fulfills the necessary conditions for practical applications as they unveil a strong chemical stability, high electrical resistivity, low hysteresis and mechanical stability [8, 9]. In contrast, the magnetocaloric potential of the RVO_3 vanadates (R = rare earth) has not yet been explored except for the bulk $HoVO_3$ [12]. However, perovskite-type vanadium oxides RVO_3 display a great variety of phase transitions associated with a series of charge, spin and orbital ordering phenomena making them interesting candidates from a magnetocaloric point of view.

Today's research activities on magnetocaloric thin films attract a wide interest due to their potential integration in miniaturized electronic devices [13-14]. This particularly motivated us to investigate the MCE in RVO_3 thin films since their behavior strongly depends on the cooperative nature of the Jahn-Teller distortion making them sensitive to strain effects including the induced biaxial strain due to the lattice mismatch between the substrate and the film. Such structural effects tend-to play an important role in tuning the film properties [15-16]. In this work, we mainly focus on exploring and tuning the magnetic and magnetocaloric properties of high quality epitaxial $PrVO_3$ (PVO) thin films by applying a compressive strain via a proper choice of substrate.

$PrVO_3$ thin films were grown by pulsed-laser deposition on two different cubic substrates, namely, (001)-oriented (La,Sr)(Al,Ta) O_3 (LSAT) and (001)-oriented $SrTiO_3$ (see experimental and methods). To investigate the strain effect on the magnetic properties of $PrVO_3$ thin films, the magnetization dependence on temperature was measured for PVO/$SrTiO_3$ under an applied magnetic field of 50 Oe as shown in Figure 1. Hysteretic loop is also performed at 10 K in magnetic fields changing between –6 and 6 T (see the inset of Figure 1). To ensure a perfect demagnetization, our sample was heated above T_N and cooled down to the desired temperature before each run. Magnetic measurements indicate hard-ferromagnetic behavior below 80 K similar to that reported previously for bulk PVO [17-19]. In fact, the S-shape of magnetization depicts a metamagnetic transition which is defined as the transition between antiferromagnetic (AF) and ferromagnetic (F) configurations of spins under the effect of magnetic fields or temperature change [20]. The intrinsic coercivity is $\sim$ 2.8 T while the remanence magnetization is $\sim$ 48 emu/cm^3. The magnetization saturation is found to be $\sim$ 54 emu/cm^3 being equivalent to 0.291 μ_B/ f.u at 10 K.

The presence of soft component can be seen at a magnetic field of ~ 0.2 T indicated by the shape of M vs H loop caused by the magnetic field induced transition which is absent at higher temperatures as earlier observed in ref. [21] The high coercivity may arise from the pinning mechanism due to the microstructure as well as the film unit cell orientation compared to the in-plane and out-of plane magnetic field directions. On the other hand, we observed a reduction of T_N compared to bulk PVO ($T_N \approx 140$ K) which could be explained by the oxygen vacancy-induced film lattice distortion [20]. XRD reveals that the pseudo cubic volume of PVO unit cell when deposited on $SrTiO_3$ ($\simeq 60.91$ Å^3) is larger than its equivalent of the bulk ($\simeq 58.86$ Å^3) [22]. As a result, the volume expansion decreases the transfer integral which tends to reduce the neighbor exchange interactions as the magnetic interactions in this system are governed by super exchange mechanisms. It is worthy to mention that no significant magnetic anisotropy is observed when comparing the performed magnetic measurement under magnetic fields applied in and out of the sample plane.

Figures 2c-d display some selected isothermal magnetization curves for two different orientations measured up to 6 T of a PVO film deposited on a (001)-oriented LSAT substrate. As shown, the magnetization saturation is markedly enhanced when compared to PVO/$SrTiO_3$, reaching about $\simeq 900$ emu/cm^3 and $\simeq 785$ emu/cm^3 at 3 K for $H\perp$ (Figure. 2d) and H// (Figure. 2c), respectively. At 10 K, the corresponding magnetization saturations are about $\simeq$ 402 emu/cm^3 and $\simeq 305$ emu/cm^3, respectively. These values are much larger than those of $PVO/SrTiO_3$ as can be clearly seen from the inset of Figure 1. In addition, the coercive field is largely reduced to attain about 0.3 T and 1.1 T for hysteretic loops performed in plane and out of plane (Figure 2), respectively. More surprisingly, the coercive field decreases dramatically at 3 K reaching only 0.05 T for magnetic fields applied within the films plane as shown in Figure 2.d. This markedly contrasts with the conventional magnets in which usually the thermal excitations lead to the reduction of coercivity. This contrast could be attributed to

FM and AFM couplings or/and the spin and orbital transitions usually leading to stair-like hysteresis observed in bulk $PrVO_3$[18]. The enhancement of coercivity when heating may also be attributed to the stress induced magnetic anisotropy due to the relaxation of the surface stress reported for various magnetic thin films [23]. The temperature dependence of magnetization at an in-plane applied magnetic field of 50 Oe is displayed in Figure 2a. As can be clearly observed, we can see a sharp decrease of magnetization at low temperature and a magnetic transition from paramagnetic (PM) to an antiferromagnetic (AFM) phase transition occurs at $T_N = 125$ K. Such a transition is attributed to the beginning of a G-type spin ordering (G-SO) [17]. The differentiation of the temperature-dependent magnetization is displayed in the inset of Figure 2a where two additional magnetic transitions take place at $T_2 \simeq 20$ K and $T_3 \simeq 80$ K. These transitions were absent in bulk PVO [24] but they were recently reported in strained PVO films [21] and in doped $Pr_{1-x}Ca_xVO_3$ compounds [25]. Upon cooling down to 3 K, the plot of the first derivative of the magnetization temperature dependence exhibits a minimum at very low temperature which could be explained by the polarization of the praseodymium magnetic moments. The newly established order is due to the fact that the antiferromagnetic vanadium sublattice produces an exchange field that results in a ferrimagnetic structure of Pr sublattice under cooling as already observed in other vanadates [25]. This is supported by the presence of a soft component at temperatures below 20 K (Figure 2c) and also by the fact that the magnetization saturation reaches 4.86 and 5.54 μ_B at 3 K when a magnetic field is applied in and out-of-plane, respectively. On the other hand, these findings inform us on the contribution of both Pr^{3+} and V^{3+} ions to the whole magnetization since the theoretical saturated moment of free Pr^{3+} and V^{3+} ions are 3.22 and 2.12 μ_B suggesting that all the praseodymium and vanadium moments are fully aligned parallel to the magnetic field.

The ZFC, FCW and FCC curves were measured in 50 Oe field from 3 to 300 K for $PVO/LSAT$ as shown in Figure 2b. The bifurcation between FC and ZFC magnetizations indicates an intrinsic disorder and irreversibility being the characteristic of a complex system. This difference reflects the impact of the anisotropy on the shapes of ZFC and FC curves below the ordering temperature since the coercivity is related to the magnetic anisotropy. The latter plays an important role in determining the magnetization at a given field strength during both the ZFC and FC processes since it aligns the spins in a preferred direction. During the ZFC process, the spins are locked in random directions since no magnetic field is applied while cooling the thin films to the desired temperature. When a small magnetic field is applied at temperatures far below T_N and as the system is anisotropic [26], the magnetization decreases to reach negative values indicating a possible competition between antiferromagnetic interactions, a characteristic which is observed in orthovanadate RVO_3 compounds [27]. A small negative trapped field in the sample space as well as the coercivity could be responsible for the negative magnetization [28]. During the FC process, the PVO film is cooled under the application of a magnetic field. Therefore, the spins will be aligned in a specific direction depending on the strength of the applied magnetic field. Consequently, M_{FC} continuously increases below T_N as the temperature decreases.

Magnetic isotherms collected under magnetic fields going from 0 up to 6 T at different temperatures are reported in Figures 3a-b for the $PVO/LSAT$ films. Except the isothermal magnetization at 3 K which shows a typical behavior of a ferromagnetic material, all the other isotherms follow a sharp increase when the magnetic field is below 30 kOe indicating a field induced first order metamagnetic transition from AFM to FM state as a result of the strong competition between Pr 4f and V 3d spins [21,31]. Such a competition often leads to a giant MCE in strongly correlated materials [29-31]. A similar behavior is found in the corresponding Arrot plots (M^2 versus H/M) confirming the first order nature of the transition according to Banerjee [36] criterion as the curves show negative slope at some points (not shown here).

The large field-induced metamagnetic transition in $PVO/LSAT$ films and the soft component in M vs H below 30 K are a clear indication of a possible giant magnetic entropy change. In order to explore the magnetocaloric effect in PVO films, magnetic field-induced entropy change $-\Delta S_M$ was calculted from magnetic isotherms by using the well-known Maxwell relation (MR) given as follow:

$$\Delta S_M = \int_0^H \left(\frac{\partial M}{\partial T}\right)_H dH$$

We are aware that the utilization of Maxell relation to evaluate entropy changes in materials showing large hysteretic effects could lead to spurious values as already demonstrated by one of the present paper authors [32]. However, the Maxwell relation can be also used to reasonably evaluate the MCE in term of the entropy change even in first-order phase transition materials provided that the remaining magnetization from previous isotherms is suppressed via a thermal loop [33]. On the other hand, it has been demonstrated recently that the magnetocaloric effect in multiferroics could be evaluated perfectly via Maxwell relation [34]. In this way, it has been particularly found that the deduced entropy change from magnetization measurements of $EuTiO_3$ fits perfectly with that obtained from specific heat data [34].

In our case, magnetic isotherms of Figure 3a-b are used to calculate the entropy change exhibited by the PVO films on $LSAT$. However, since the entropy change is proportional to the aera between two successive isotherms, ΔS_M was directly calculated without subtracting the magnetic contribution arising from the substrate as already done in the case of La_2NiMnO_6 thin films [35]. For PVO/STO, it was difficult to calculate the MCE because of the overlap between M vs H curves (see Supplementary material) at low temperatures.

The temperature dependence of the magnetic entropy change unveils larger values at very low temperature for $PVO/LSAT$ films. $-\Delta S_M$ reaches roughly a maximum value of 56.7 J.$kg^{-1}.K^{-1}$ for a magnetic field changing from 0 to 6 T applied in the sample plane (Figure

3a), being about 63% of its theoretical limit given by R*Ln(2J+1). In a similar field change applied out of plane(Figure 3b), $-\Delta S_M$is slightly lower and found to be about 52.7 J.$kg^{-1}.K^{-1}$. Also, the magnetic entropy change shows a large magnetocaloric effect under relatively low magnetic fields that can be easily reached via permanent magnets. In the magnetic field change of 2 T applied within and out of thin films plane, $-\Delta S_M$ reaches 19.5 and 16.3 J.$kg^{-1}.K^{-1}$, respectively. As shown in Figures 3b-c, a large magnetocaloric effect can be induced below the AFM transition temperature. This suggests that a major part of the contribution to the MCE comes from the praseodymium 4f spins.

A list of some relevant magnetocaloric materials working in the cryogenic temperature range are reported in Table 1 for comparison. As shown, the exhibited ΔS_M by the strained PVO film is significantly larger than its equivalent reported for several rare-earth metal transition oxides making the PVO films potential candidates for low temperature magnetic refrigeration.

Theoretical calculations are important for a better understanding of the fundamental mechanisms behind the physical properties of materials. Here, ab initio calculations based on the density functional theory (DFT) were performed to investigate the magnetic and magnetocaloric features of both bulk and thin films of PVO. In order to check the ground state of bulk PVO, the total energies of four different magnetic ordering configurations are calculated using GGA+U approximation. The ferromagnetic (FM) and the three antiferromagnetic (AFM) structures are shown in Figure 4a and denoted by AF-G, AF-C and AF-A. Our results indicate a ground state magnetic structure where the vanadium spins form a C-type AFM structure being consistent with previous studies [17-21]. For thin films calculations, two different orientations have been taken into account. First, we preserve the bulk Pbnm symmetry for a growth along the [001] direction where the two lattice vectors of the orthorhombic unit cell lie within the substrate plane. A second growth along the orthorhombic [110] direction where the compressive constraint lowers the symmetry to $P2_1/m$ is also considered. The latter scenario

that results in monoclinic unit cell was found to be clearly preferable by comparing the total energy difference between the two symmetries. It yields to G-type spin ordering for PVO grown on both $LSAT$ and STO substrates.

The enhancement of magnetic interactions under compressive strains is also seen when using DFT calculations. The intraplane and interplane magnetic exchange interactions J_{intra} and J_{inter} can be determined from the relation between the exchange parameters $J_{i,j}$ and the magnetic energies $e_{i,j}$ of four magnetic configurations, $e_{i,j} = J_{i,j}. S_i S_j$ based on the effective Heisenberg model H= $\sum_{i,j} J_{i,j}. S_i S_j$ where S_i takes 1 restricted to nearest neighbor vanadium sites (Figure 4b). As shown, the intraplane magnetic exchange interactions increase due to the compressive strain effect along the [110] direction. In fact, the film lattice parameters tend to match those of the substrate leading to an increase in the out-of-plane lattice parameter. This can be clearly seen when plotting the c/a sub ratio for two orientations as a function of lattice parameter a_{sub} of the substrate (See inset of Figure 4b). It is worth noting that some of Pr-V pairs are found to interact ferromagnetically confirming the competition between AFM and FM interactions.

To sum up, we have investigated the magnetic and magnetocaloric properties of PVO films grown by pulsed laser deposition, in view of their potential application in cryogenic magnetic cooling. The obtained results reveal that the magnetic and magnetocaloric properties of PVO compounds can be easily tailored by using the thin films approach. Particularly, the coercive magnetic field was dramatically decreased making from the PVO compound a nearly soft magnet. Accordingly, a giant MCE is exhibited by PVO thin films grown on $LSAT$ substrates at low temperatures pointing out the great impact of strain effects and the competition between AFM and FM exchange interactions. This finding would open the way for the implementation of PVO thin films in some specific applications such as on-chip magnetic micro-refrigeration

and sensor technology. On the other hand, DFT calculations have confirmed the ground state and the enhancement of magnetic interactions via compressive strains in PVO thin films.

Our result not only suggests that epitaxial PVO thin films present a non-negligible potential for refrigeration at cryogenic temperatures but may also pave the way for new applications taking for example advantage of the possibility to tailor the magnetic coercivity in PVO thin films. However, we are aware that the reported entropy change values in PVO thin films are too large when compared to the best magnetocaloric materials working in a similar working temperature range. The necessary was done to reasonably evaluate the MCE in term of the entropy change by considering the impact of hysteretic phenomena. However, in order to accurately estimate ΔS, the measurements of specific heat in equilibrium conditions are highly required. This point will be certainly addressed in the future.

EXPERIMENTS AND METHODS

***EXPERIMENTS*:** The epitaxial PVO films were grown by pulsed-laser deposition (PLD) on two different cubic substrates, namely, (001)-oriented (La,Sr)(Al,Ta)O_3 (LSAT) and (001)-oriented $SrTiO_3$ (STO). Their in and out-of-plane lattice parameter are found to be 3.868 Å and 3.95 Å with a thickness of 41.7 nm for the $LSAT$ film while those of the $SrTiO_3$ film are 3.905 Å and 3.92 Å with a thickness of 100 nm. The films deposition was carried out with a KrF excimer laser (λ = 248 nm) with a repetition rate of 2 Hz and a laser fluence of ~ 2 J/cm^2 focusing on stoichiometric ceramic targets. The thin films were deposited at an optimum growth temperature (T_{GROWTH}) of 650 °C and under oxygen partial pressure (P_{GROWTH}) of 10^{-6} bar.

In ZFC measurements our sample was cooled to the desired temperature without the application of a magnetic field, then data were collected while heating under magnetic field. For the FC process, the sample was cooled in the presence of an external magnetic field to the desired

temperature. We performed two modes, field cooled cooling (FCC) and field cooled warming (FCW) where data are collected during the cooling and heating processes, respectively.

The in-plane and out-of-plane magnetizations were performed by using the Quantum Design SQUID-VSM. Each hysteresis loop was measured after a 150 K excursion above the Néel temperature and corrected by subtracting the diamagnetic contribution arising from the substrate.

THEORY: Based on the density functional theory (DFT), first principles calculations were performed using Vienna Ab Initio simulation Package [37-39] with the PBE functional used to reproduce the electronic exchange correlation while the projector augmented-wave (PAW) was employed to construct the pseudopotential of all involved species. We performed a U correction of 3.5 eV [41] to deal with the strong on-site Coulomb interaction of 3 d electrons. The cut-off energy set to 500 eV and a k-points shell of 6x6x6 according to the Monkhorst-Pack grid was used for orthorhombic structures which is found to yield a better convergence. For bulk calculations, all cell parameters and atomic positions are relaxed within Pbnm symmetry. In order to study the effect of epitaxial strain arising from the film/substrate lattice mismatch, bulk geometry has been subjected to an epitaxial constraint on its lattice parameters. Two different growth orientations are considered. The first growth is along the Pbnm [001] direction where the two lattice vectors of the orthorhombic unit cell lie within the substrate plane with a = b = $\sqrt{2}a_{sub}$ (a_{sub} = substrate lattice) to preserve the Pbnm symmetry of the bulk PVO. The second growth is considered along the orthorhombic [110] direction where the compressive constraint lowers the symmetry to $P2_1/m$ resulting in a monoclinic cell unit with $\gamma \neq 90°$. The in-plane lattice parameters are set equal to the lattice constant of the substrate, while the out-of-plane parameter is optimized for each value of the substrate parameter and all the structures are

relaxed until the forces on atoms were less than 3 meV/Å . Four magnetic states are considered in the simulation (Ferromagnetic, G-type, C-type, and A-type antiferromagnetic).

Acknowledgements
This work was supported by PHC Toubkal 17/49 project. M. Balli highly appreciates the financial support from the International University of Rabat.

References

[1] M. S. Song, K. K. Cho, B. Y. Kang, S. B. Lee & B. K. Cho. Sci Rep. **2020,** 10, 803.
[2] S. Murakami, N. Nagaosa, Phys. Rev. Lett. **2003**, 90, 197201.
[3] Y. Tokura, Rep. Prog. Phys. **2006**, 69, 797.
[4] Taguchi, Y., Sakai, H., Choudhury, D., Adv. Mater. **2017**, 29, 1606144.
[5] D. Choudhury, T. Suzuki, D. Okuyama, D. Morikawa, K. Kato, M. Takata, K. Kobayashi, R. Kumai, H. Nakao, Y. Murakami, M. Bremholm, B. B. Iversen, T. Arima, Y. Tokura, Y. Taguchi, Phys. Rev. B **2014**, 89, 104427.
[6] N. H. Dung, Z. Q. Ou, L. Caron, L. Zhang, D. T. Cam Thanh, G. A. de Wijs, R. A. de Groot, K. H. J. Buschow, E. Brück, *Adv. Energy Mater.* **2011**, **1**, 1215.
[7] M. Balli, S. Jandl, P. Fournier, and A. Kedous-Lebouc, *App. Phy. Rev.* **2017**, **4**, 021305.
[8] O. Tegus, E. Brück, K. H. J. Buschow, and F. R. de Boer, Nature. **2002**, 415, 150.
[9] G. V. Brown J. App. Phy. **1976**, 47, 3673.
[10] M. Balli, S. Jandl, P. Fournier, and M. M. Gospodinov, Appl. Phys. Lett. **2014**, 104, 232402.
[11] M. H. Phan and S. C. Yu, J. Magn. Magn. Mater. **2007**, 308, 325.
[12] M. Balli, B. Roberge, S. Jandl, P. Fournier, T. T. M. Palstra, and A. A. Nugroho, J. Appl. Phys. **2015**, 118, 073903.
[13] X. Moya, L. E. Hueso, F. Maccherozzi, A. I. Tovstolytkin, D. I. Podyalovskii, C. Ducati, L. C. Phillips, M. Ghidini, O. Hovorka, A. Berger, M. E. Vickers, E. Defay, S. S. Dhesi, and N. D. Mathur, Nat. Mater. **2013**, 12, 52.
[14] Y. Liu, C. Phillips, R. Mattana, M. Bibes, A. Barthélémy and B. Dkhil. Nat. Comm. **2016**, 7, 11614 .

[15] R. A. Rao, D. Lavric, T. K. Nath, C. B. Eom, L. Wu, and F. Tsui, Appl. Phys. Lett. **1998,** 73, 3294.
[16] M.Chen, S. Bao, Y. Zhang, Y. Wang, Y. Liang, J. Wu, T. Huang, L. Wu, P. Yu, J. Zhu, Y. Lin, J. Ma, C.W. Nan, A. J. Jacobson, and C. Chen. Appl. Phys. Lett. **2019**, 115, 081903
[17] O. Copie, J. Varignon, H. Rotella, G. Steciuk, P. Boullay, A. Pautrat, A. David, B. Mercey, P. Ghosez, W. Prellier, Adv.Mater. **2017**, 29, 1604112.
[18] L. D. Tung, Phy. Rev. B, **2005**, 72, 054414.
[19] F. Wang, J. Zhang, P. Yuan, Q. Yan, P. Zhang, J. Phys.: Condens. Matter, **2000**, 12, 3037.
[20] S. Chikazumi, Physics of Ferromagnetism, Oxford University Press Inc., New-York, **1991.**

[21] D. Kumar, A. David, A. Fouchet, A. Pautrat, J. Varignon, C. U. Jung, U. Lüders, B. Domengès, O. Copie, P. Ghosez, and W. Prellier, Phys. Rev. B, **2019**, 99, 224405.
[22] O. Copie, H. Rotella, P. Boullay, M. Morales, A. Pautrat, P.-E. Janolin, I. C. Infante, D. Pravathana, U. Lüders, and W. Prellier, J. Phys.: Condens. Matter, **2013** 25, 492201.
[23] N. Anuniwat, M. Ding, S. J. Poon, S. A. Wolf, and J. Lu, J. Appl. Phys. **2013**, 113, 43905.
[24] S. Miyasaka, Y. Okimoto, M. Iwama, Y. Tokura, Phys. Rev. B. **2003**, 68, 100406.
[25] M. Reehuis, C. Ulrich, P. M. Abdala, P. Pattison, G. Khaliullin, J. Fujioka, S. Miyasaka, Y. Tokura, B. Keimer, Phys. Rev. B. **2016**, 94, 104436.
[26] P A Joy., P S Anil Kumar. and S K Date J. Phys. Condens. Matter 1998, 10, 11049.
[27] L. D. Tung, M. R. Lees, G. Balakrishnan, and D. McK. Paul, Phys. Rev. B, 2007, 75, 104404.
[28] N. Kumar and A. Sundaresan, Solid State Commun. **2010**, 150, 1162.
[29] A. Midya, P. Mandal, S. Das, S. Banerjee, L. S. S. Chandra, V. Ganesan, and S. R. Barman, Appl. Phys. Lett. **2010**, 96, 142514.
[30] M. Shao, S. Cao, S. Yuan, J. Shang, B. Kang, B. Lu, and J. Zhang, Appl. Phys. Lett. **2012**, 100, 222404.
[31] A. Midya, N. Khan, D. Bhoi, and P. Manda, Appl. Phys. Lett. **2013**, 103, 092402.
[32] M. Balli, D. Fruchart, D. Gignoux, and R. Zach, Appl. Phys. Lett. **2009**, 95, 072509.
[33] L. Caron, Z. Q. Oub, T. T. Nguyen, D. T. Cam Thanh, O. Tegus, E. Bruck, J. Magn. Magn. Mater. **2009**, 321, 3559.
[34] A. Midya, P. Mandal, K. Rubi, R. Chen, J. S. Wang, R.Mahendiran, G. Lorusso, and M. Evangelisti, Phys.Rev.B **2016**, 93,094422.
[35] D. Matte, M. de Lafontaine, A. Ouellet, M. Balli, and P. Fournier**,** Phys. Rev. App. **2018**, 9, 054042.
[36] B. K. Banerjee, Phys. Lett. **1964**, 12, 16.
[37] R. A. Rao, D. Lavric, T. K. Nath, C. B. Eom, L. Wu, and F. Tsui. Appl. Phys. Lett. **1998**, 73, 3294.
[38] G. Kresse & J. Hafner, Ab initio molecular dynamics for liquid metals. Phys. Rev. B **1993**, 47, 558.
[39] P.E. Blochl. Projector augmented-wave method. Phys. Rev. B. **1994**, 50, 17953_17979.
[40] G. Kresse & J. Furthmuller, Phys. Rev. B. **1996**, 54, 11169.
[41] S. L. Dudarev, G. A. Botton, S. Y. Savrasov, C. J. Humphreys, A. P. Sutton, Phy. Revi. B. **1998**, 57, 1505.
[42] M. Das, S. Roy, and P. Mandal. Phys. Rev. B. **2017**, 96, 174405.

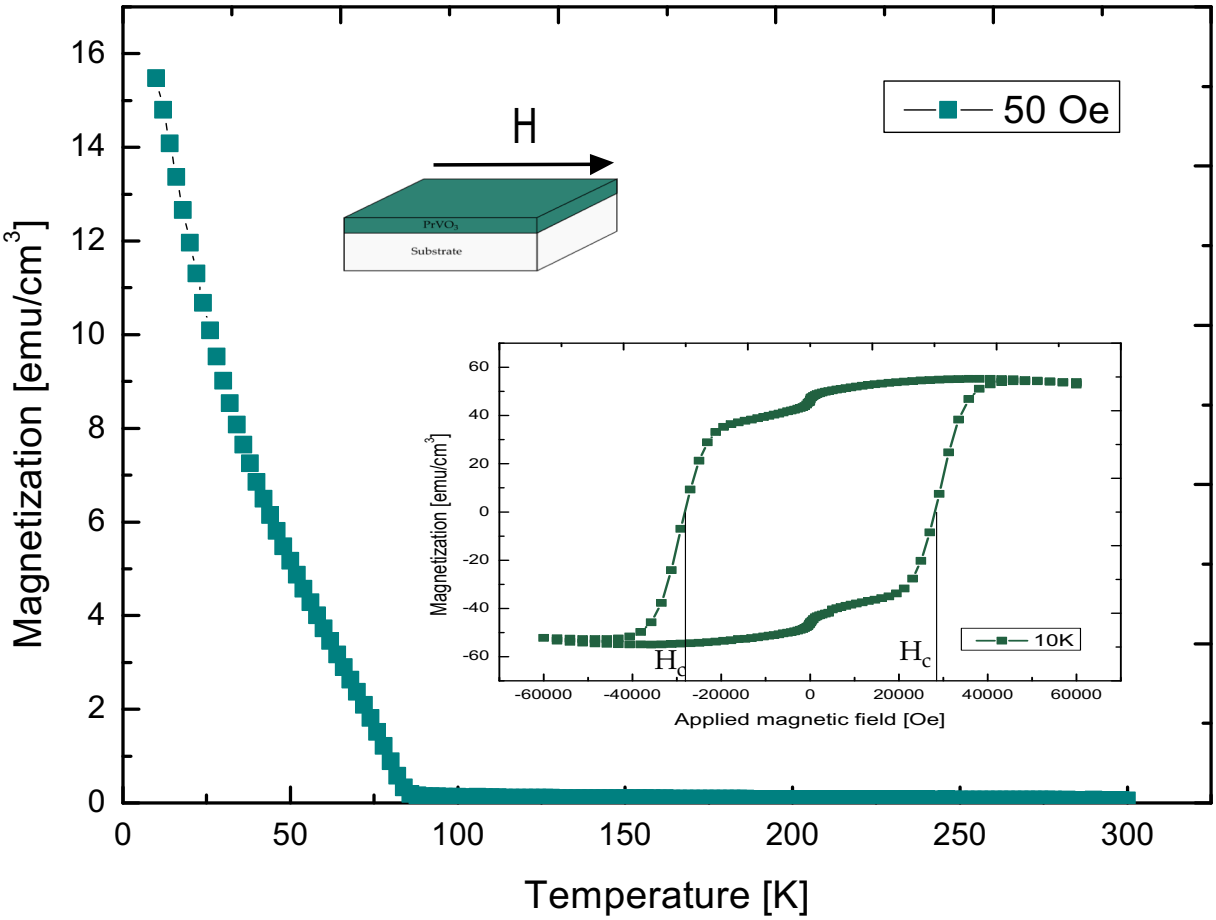

Figure 1. Magnetization dependence of temperature for $PrVO_3$ film on $SrTiO_3$ substrate performed under an in-plane applied magnetic field of 50 Oe. Inset displays the magnetic hysteresis loops measured at 10 K after subtracting the diamagnetic contribution of the substrate and the holder.

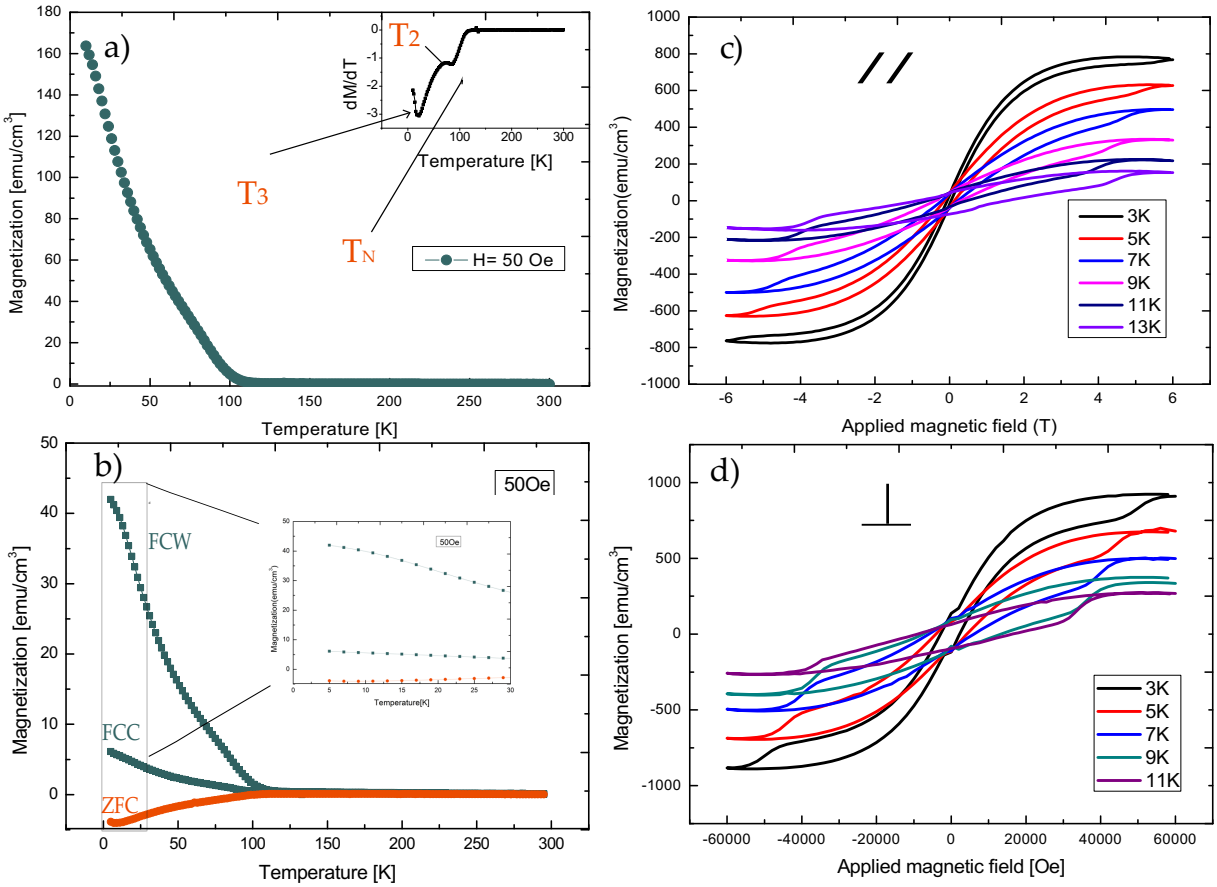

Figure 2. (a) Temperature dependence of magnetization of PrVO_3 on LSAT thin film under an in-plane applied magnetic field of 50 Oe. Inset: differentiation of the temperature-dependent magnetization. (b) Temperature dependence of magnetization in zero field-cooling (ZFC), field cooled cooling (FCC) and field cooled warming (FCW) conditions. (c, d) Some selected magnetic isotherms in the temperature range 3-13 K for PVO/LSAT collected in-plane (c) and out-of-plane (d) applied magnetic field.

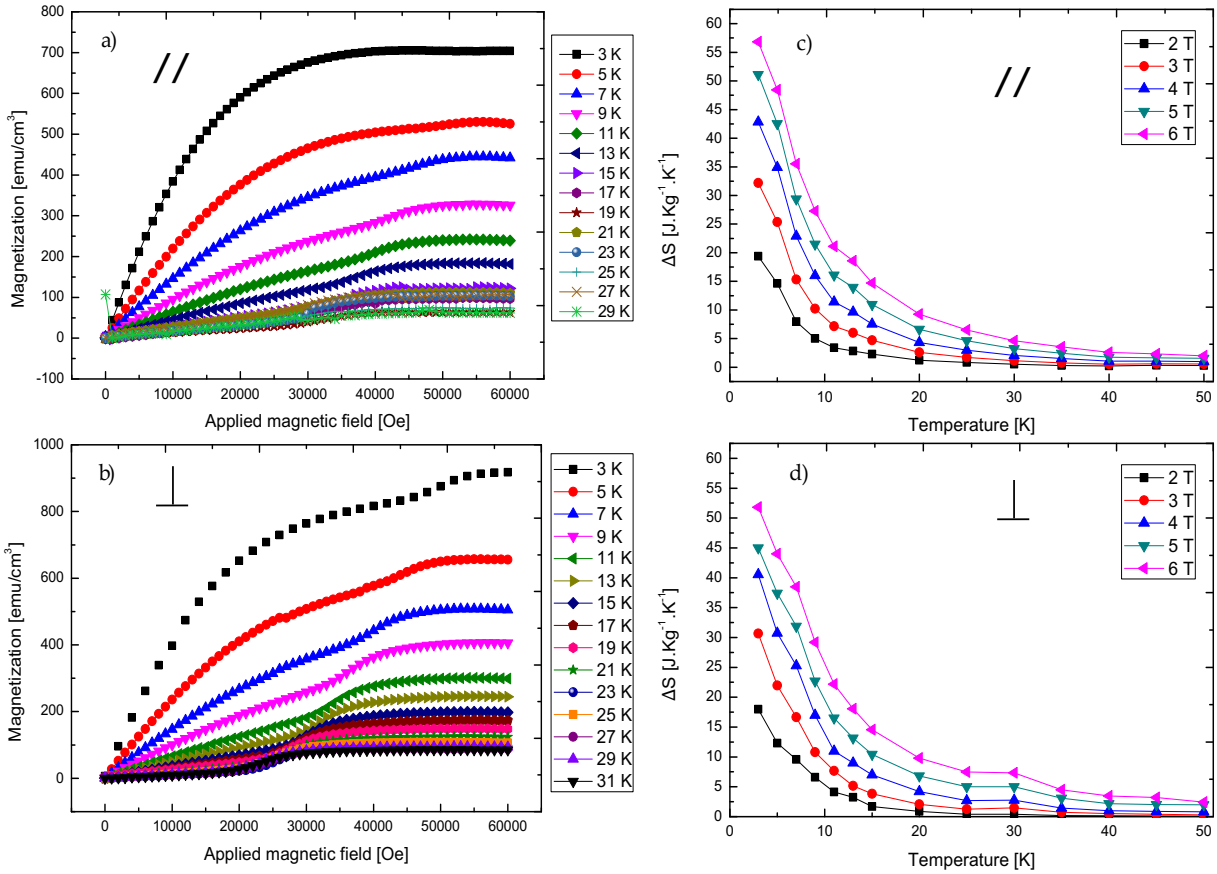

Figure 3. Magnetic and MCE properties of $PrVO_3$ on LSAT. a) Magnetic isotherms in the temperature range of 3-31 K with a step of 2 K under an in-plane (a) and out-of-plane (b) magnetic field. Each magnetic isotherm was measured after thermal excursion above T_N to ensure a perfect demagnetization of the sample and corrected for diamagnetic background signal. (c, d) Temperature dependence of magnetic entropy change of $PrVO_3$/LSAT under some selected magnetic fields applied within (c) and out-of-plane (d).

.

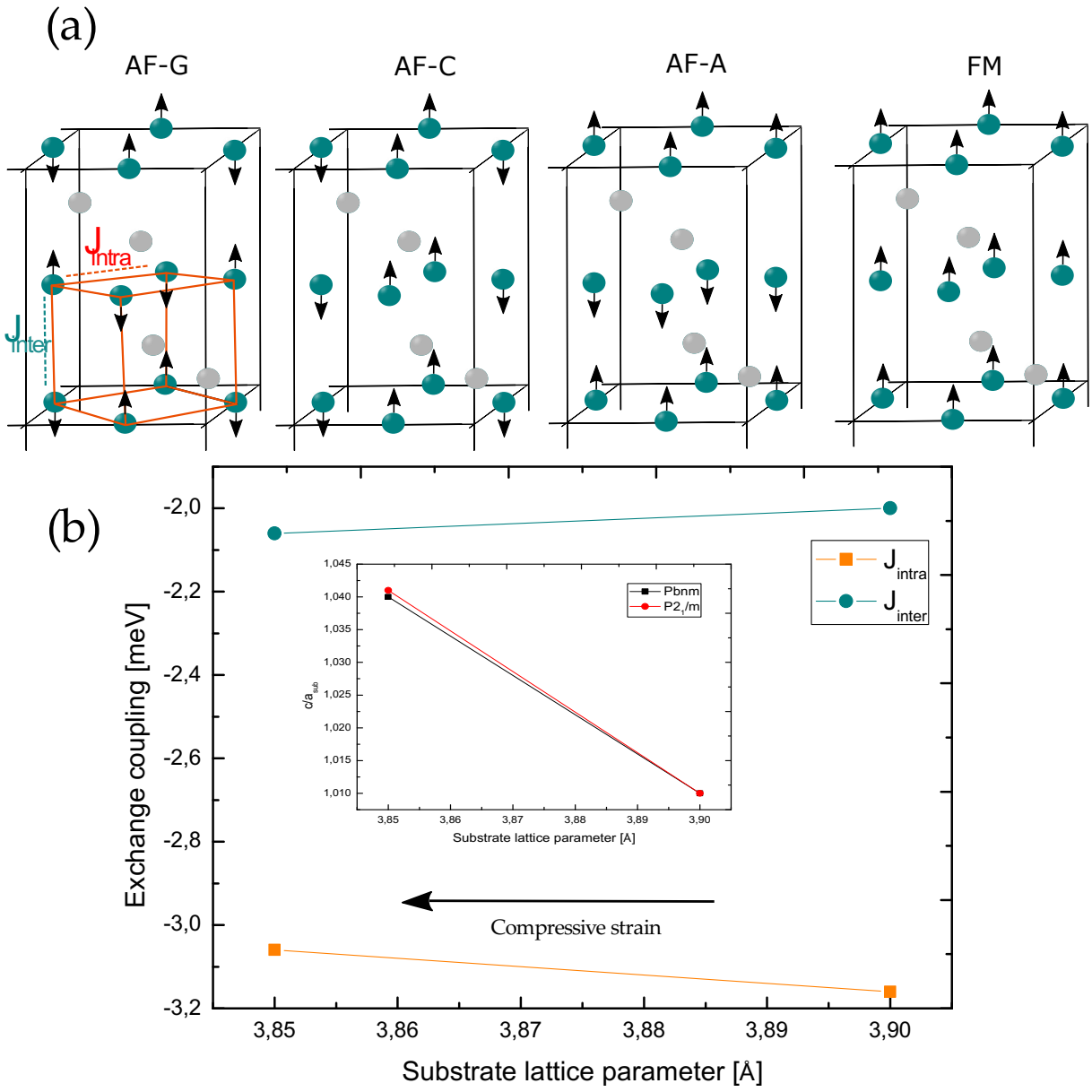

Figure 4. a) Distorted perovskite magnetic structure of PrVO_3 in which the pseudocubic cell is shown by orange lines. Four magnetic structures are schematically shown: Ferromagnetic (FM), C-type antiferromagnetic, G-type antiferromagnetic and A-type ferromagnetic. The grey and green spheres represent Pr and V atoms, respectively. b) Exchange coupling versus the lattice parameter related to STO and LSAT substrates. Inset shows the c/a_{sub} ratio for two orientations as a function of lattice parameter a_{sub} of the substrate.

Table 1. Maximum magnetic entropy change ΔS_M shown by $PrVO_3$ deposited on LSAT substrate compared to some relevant cryomagnetocaloric compounds. SC means single crystal

Materials	T(K)	ΔH (T)	ΔS (J/kg K)	Ref.
PVO/LSAT (//-⊥)	3	6 T	56.7-52.7	Present work
$GdFeO_3$ (SC)	2.5	6 T	43.1	42
$EuTiO_3$	5.6	5 T	42.4	34
$HoVO_3$ (SC)	15	7 T	17.2	12

Supporting Information

Engineering the magnetic and magnetocaloric properties of epitaxial oxide thin films by strain effects

Hamza Bouhani, Asmaa Endichi, Deepac Kumar, Olivier Copie, Halima Zaari, Wilfrid Prellier, Adrien David, Arnaud Fouchet, Omar Mounkachi, Mohamed Balli, Abdelilah Benyoussef, Abdallah El Kenz and Stéphane Mangin

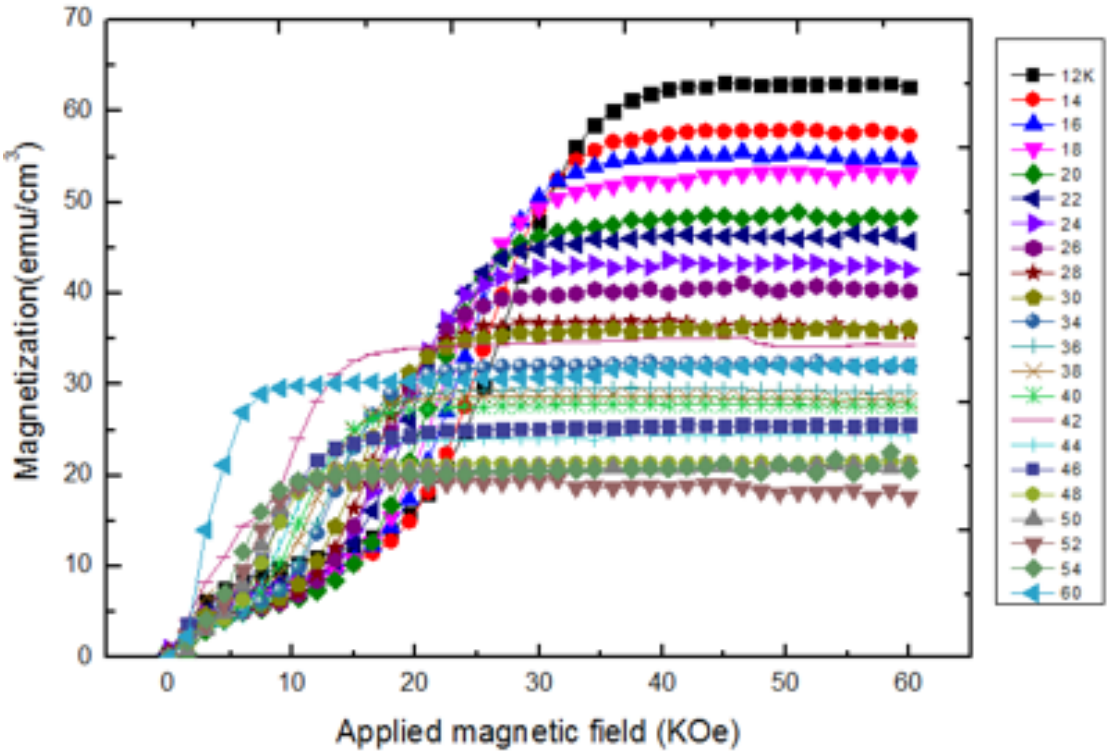

Figure S1. Magnetic isotherms of PVO on STO with a magnetic field applied within the sample plane in the range of 12 to 60 K.